Ion Channel Inhibitors

International Edition: DOI: 10.1002/anie.202000247
German Edition: DOI: 10.1002/ange.202000247

Redox Stability Controls the Cellular Uptake and Activity of Ruthenium-Based Inhibitors of the Mitochondrial Calcium Uniporter (MCU)

*Joshua J. Woods, James Lovett, Barry Lai, Hugh H. Harris, and Justin J. Wilson**

Abstract: *The mitochondrial calcium uniporter (MCU) is the ion channel that mediates Ca^{2+} uptake in mitochondria. Inhibitors of the MCU are valuable as potential therapeutic agents and tools to study mitochondrial Ca^{2+}. The best-known inhibitor of the MCU is the ruthenium compound Ru360. Although this compound is effective in permeabilized cells, it does not work in intact biological systems. We have recently reported the synthesis and characterization of Ru265, a complex that selectively inhibits the MCU in intact cells. Here, the physical and biological properties of Ru265 and Ru360 are described in detail. Using atomic absorption spectroscopy and X-ray fluorescence imaging, we show that Ru265 is transported by organic cation transporter 3 (OCT3) and taken up more effectively than Ru360. As an explanation for the poor cell uptake of Ru360, we show that Ru360 is deactivated by biological reductants. These data highlight how structural modifications in metal complexes can have profound effects on their biological activities.*

Introduction

Mitochondrial calcium ion (Ca^{2+}) trafficking is essential for proper cellular function, as it plays a key regulatory role in many bioenergetic processes.[1] Uptake of these ions by the mitochondria is mediated by the highly selective and inwardly rectifying channel known as the mitochondrial calcium uniporter (MCU).[2] This protein resides in the inner mitochondrial membrane (IMM) and forms a tetrameric, dimer of dimers type of assembly,[3–6] with both the N- and C-terminal domains located within the mitochondrial matrix.[7,8] Although mitochondrial Ca^{2+} uptake through the MCU is needed for proper cellular function, dysregulation of this process through mitochondrial calcium overload gives rise to cell damage and death. This improper handling of Ca^{2+} ions by the mitochondria manifests in the form of several pathological conditions, including cardiovascular disease,[9,10] stroke,[11] neurodegeneration,[12] and cancer.[13] As such, the MCU has arisen as a valuable therapeutic target and has been the subject of intense study by researchers seeking to more precisely understand the role of this transporter in disease.[14–18]

Despite the significance of the MCU in human disease, chemical tools and potential therapeutic agents that can modulate its Ca^{2+}-uptake properties are limited.[19] In fact, extensive efforts to develop selective and cell-permeable inhibitors of the MCU have only recently been initiated. Within the last four years, several new small-molecule inhibitors of the MCU have been discovered. These compounds, KB-R7943,[20] mitoxantrone,[21] DS16570511,[22] NecroX-5,[23,24] and minocycline,[25] bear little structural resemblance to one another, a feature that reflects the difficulty in rationally designing effective MCU inhibitors. Furthermore, all of these compounds are known to exhibit a primary biological function that is distinct from MCU inhibition.[20,26–30] For example, the MCU inhibitors mitoxantrone and DS16570511, which were discovered via high throughput compound library screening,[21,22] are more commonly known for their abilities to hyperpolarize mitochondria[31] and inhibit human topoisomerase II, respectively.[29,32] These off-target effects hamper the use of these small-molecule MCU inhibitors as potential drug candidates and as tools for probing the role of the MCU in pathological conditions.

The most widely used MCU inhibitor is ruthenium 360 (Ru360, Scheme 1), a binuclear oxo-bridged Ru compound that is named for its strong UV-visible absorbance feature at 360 nm.[33–35] Ru360 selectively inhibits MCU-mediated mitochondrial Ca^{2+} uptake with nanomolar potency in permeabilized cells, without affecting the activity of Na^+/Ca^{2+} channels.[35] Its potent MCU-inhibitory activity was applied in vivo to protect rat hearts subjected to ischemia reperfusion injury.[36,37] Despite these promising results, the more widespread use of this compound in intact biological systems is significantly limited by its poor cell permeability.[35,38] Furthermore, Ru360 is of limited commercial availability, and its synthesis requires a challenging, non-routine purification procedure.

To address the deficiencies of Ru360, our group has been developing new structural analogues of this compound and exploring their biological activities.[39–42] We have shown that the compound Ru360′ (Scheme 1), where the axial formate

[*] J. J. Woods, Prof. J. J. Wilson
Department of Chemistry and Chemical Biology, Cornell University
Ithaca, NY 14853 (USA)
E-mail: jjw275@cornell.edu

J. J. Woods
Robert F. Smith School for Chemical and Biomolecular Engineering, Cornell University, Ithaca, NY 14853 (USA)

J. Lovett, Prof. H. H. Harris
Department of Chemistry, The University of Adelaide
Adelaide, SA, 5005 (Australia)

Dr. B. Lai
Advanced Photon Source, X-ray Science Division, Argonne National Laboratory, Argonne, IL 60439 (USA)

Supporting information and the ORCID identification number(s) for the author(s) of this article can be found under https://doi.org/10.1002/anie.202000247.

 © 2020 Wiley-VCH Verlag GmbH & Co. KGaA, Weinheim

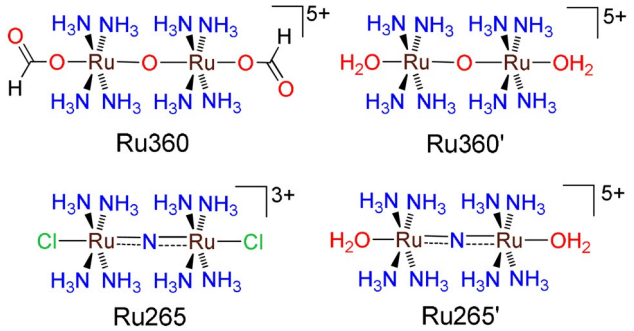

Scheme 1. Chemical structures of Ru360 and the compounds Ru360′, Ru265, and Ru265′ discussed in this work.

ligands of Ru360 have been exchanged for coordinated water molecules, is capable of inhibiting mitochondrial Ca^{2+} uptake. This structural modification, however, does not confer this compound with improved the cell permeability compared to Ru360. More recently, we have identified that the nitrido-bridged diruthenium compound Ru265, named based on its electronic absorbance feature at 265 nm, maintains the high MCU-inhibitory activity of Ru360, while exhibiting significantly enhanced cellular uptake. This compound is capable of inhibiting mitochondrial Ca^{2+} uptake in intact cells, is effectively nontoxic, and can protect neonatal rat ventricular myocytes from simulated ischemic reperfusion injury.[42] Furthermore, Ru265 is selective for the MCU over related Na^+/Ca^{2+} exchange channels. Thus, Ru265 has arisen as an important chemical tool and therapeutic candidate for studying diseases related to mitochondrial Ca^{2+} dysregulation.

The cell-permeability and efficacy of Ru265 in intact cells in comparison to Ru360 and Ru360′ is unexpected given the structural similarities of these compounds. In this report, we sought to determine the factors that give rise to the high cell permeability of Ru265. These efforts have led us to explore and compare the physical properties of Ru360′ and Ru265, and to carry out detailed mechanistic cellular uptake studies. Taken together, these results suggest that the nitrido bridge of Ru265 confers this compound with enhanced redox stability, which is a key factor that mediates its cellular uptake in an intact form.

Results and Discussion

It is well established that Ru265 and Ru360 inhibit mitochondrial Ca^{2+} uptake effectively in permeabilized cells. We first sought to confirm that the observed MCU-inhibitory activity of these complexes arises from their intact forms, rather than likely impurities or decomposition products. To consider this possibility, we tested the mitochondrial calcium uptake inhibition properties of several structurally related ruthenium compounds and starting materials. Of these compounds, $K_3[Ru_2(\mu\text{-}N)Cl_8(OH_2)_2]$ and $K_4[Ru_2(\mu\text{-}O)Cl_{10}]$ are the starting materials for Ru265 and Ru360′ respectively, and the mononuclear Ru ammine complexes *cis*-$[Ru(NH_3)_4Cl_2]^+$, *trans*-$[Ru(NH_3)_4Cl_2]^+$, $[Ru(NH_3)_5Cl]^{2+}$, and $[Ru(NH_3)_6]^{3+}$ are potential decomposition products or impurities that may arise during the syntheses of Ru360′ and Ru265.

Our evaluation of mitochondrial calcium uptake inhibition employed digitonin-permeabilized HeLa cells treated with the sarco/endoplasmic reticulum inhibitor thapsigargin and the Ca^{2+}-responsive fluorescent dye Calcium Green-5 N as described previously.[39,43] The permeabilized cells were treated with the desired Ru complex (10 μM) as the chloride salt, and the fluorescence intensity of the dye was used as a direct readout of the extramitochondrial Ca^{2+} levels upon addition of a 20 μM bolus of $CaCl_2$. This relatively high concentration was chosen to screen the ability of the complexes to inhibit the MCU, regardless of how poorly potent the compound may be. In the presence of 10 μM Ru360′, Ru265, or Ru265′, an analogue of Ru265 where the axial chloride ligands have been replaced with coordinated water molecules (vide infra and Scheme 1), the addition of a Ca^{2+} bolus gives rise to an initial increase in dye fluorescence intensity that does not decrease over time, which is a consequence of the inhibition of MCU-mediated Ca^{2+} uptake by these compounds (Figure 1, S1, Supporting Information, SI). In contrast, the binuclear Ru starting materials, $K_3[Ru_2(\mu\text{-}N)Cl_8(OH_2)_2]$ and $K_4[Ru_2(\mu\text{-}O)Cl_{10}]$, and all of the mononuclear ammine complexes failed to perturb mitochondrial calcium uptake, indicating that these compounds do not possess MCU-inhibitory activity at this relatively high concentration of 10 μM (Figure 1, Figure S1, SI). It is noteworthy that $[Ru(NH_3)_6]^{3+}$ and *cis*-$[Ru(NH_3)_4Cl_2]^+$ displayed partial MCU-inhibitory activity in our initial evaluation, but recrystallization of these compounds ablated their ability to inhibit the MCU. Based on these data, we hypothesize that small amounts of Ru360 were present as impurities in these crude samples. This observation is reminiscent of how Ru360 was initially discovered to be an impurity in most formulations of the trinuclear Ru complex, RuRed, and highlights how care must be taken in identifying the species responsible for MCU inhibition.[34,44] Collectively, these results show that the MCU-inhibitory properties of Ru265, Ru265′ and Ru360′ are unique to these complexes;

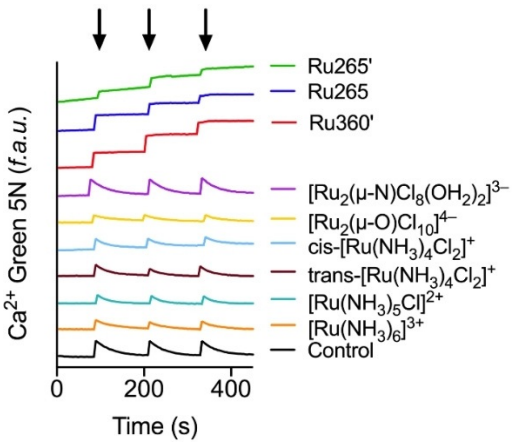

Figure 1. Changes in extramitochondrial Ca^{2+} clearance in permeabilized HeLa cells treated with the indicated Ru complex (10 μM) after addition of 20 μM Ca^{2+}. Arrows indicate time of Ca^{2+} addition.

 © 2020 Wiley-VCH Verlag GmbH & Co. KGaA, Weinheim

mononuclear analogues and anionic binuclear analogues, compounds that represent likely impurities or decomposition products, are not able to inhibit mitochondrial calcium uptake.

The solution behaviour and speciation of coordination complexes often plays a large role in their observed biological activities.[45] As such, we sought to gain insight on the solution behaviour of Ru265 in comparison to Ru360′ as means of understanding the differential efficacy of these agents in intact cells. Similar to Ru360,[34] the axial chloride ligands of Ru265 are labile and are replaced with water molecules in aqueous solution to give Ru265′ (Scheme 1). This aquation reaction was monitored by UV-vis spectroscopy by following the change in absorbance at 270 nm (Figure S2, SI). We confirmed that we were observing the aquation reaction and that it had proceeded to completion by comparing the final UV-vis spectrum of the reaction to that of Ru265 treated with an excess of $AgPF_6$ to remove all chloride from solution as insoluble AgCl (Figure S3). Although this aquation reaction is expected to be a two-step process, our kinetic analysis revealed a simple mono-exponential decay of the starting materials. As such, the aquation process was treated as a single-step, first order reaction.

The observed pseudo-first order rate constants for the aquation of Ru265 in pH 7.4 MOPS buffer at 23 and 37 °C and in the presence and absence of a physiologically relevant concentration of saline are shown in Table 1 and S1 (SI). Although we hypothesized that the reaction would be dependent on the concentration of chloride anions, no significant differences in the aquation rate constants was observed in the presence or absence of 0.1 M NaCl. At room temperature, the aquation half-life of Ru265 is ≈45 min, which decreases to ≈2 min at a physiologically relevant temperature of 37 °C (Table 1). Given this short half-life, it appears that the diaqua complex Ru265′ is the major species that enters and is present in cells. This aspect of the speciation of Ru265 is important because the complex charge difference between Ru265 (+3) and Ru265′ (+3, +4, or +5 depending on the pH of the solution) could have significant implications on its cellular uptake efficacy and subcellular localization. For comparison, Ru360′ showed no change in its absorbance spectrum after incubation in MOPS buffer for 12 h or upon treatment with 45 equivalents of $AgPF_6$. This result confirms that the axial water ligands of this compound remain unchanged, as previously reported (Figure S4, SI).[39]

Table 1: Relevant physical properties of Ru265 and Ru360.

Property	Ru265	Ru360′
Aquation rate constant ($\times 10^4$; s^{-1}; pH 7.4; 23 °C)	2.59(15)	–
$t_{1/2}$ (min; pH 7.4; 23 °C)	44.6	–
Aquation rate constant ($\times 10^4$; s^{-1}; pH 7.4; 37 °C)	4.92(66)	–
$t_{1/2}$ (min; pH 7.4; 37 °C)	2.3	–
pK_{a1}	5.14(02)	2.98(05)
pK_{a2}	7.00(11)	4.75(09)
Charge at pH 7.4	+3/+4[a]	+3
Redox events[b] (mV vs. SCE)	–	295, −239, −479, −740

[a] The two species exist in a ratio of 72:28. [b] 0.1 M NH_4HCO_2; pH 7.4; 23 °C

Water molecules that are coordinated to metal ions are generally acidic. The pK_a values of these ligands will dictate their speciation at physiological pH, and the protonation state of the coordinated water molecule will affect the reactivity of the complex and its overall charge. These properties can have a significant effect on the cellular uptake and intracellular localization of the complex. Because the diaqua complexes Ru265′ and Ru360′ are the major species present in biological systems, we sought to characterize the pK_a values of the coordinated water molecules to determine the protonation state of the complexes at physiological pH. Spectrophotometric titrations over the range of pH 1–9.5 were carried out, revealing two ionization constants that correspond to the pK_a values of the two coordinated water molecules (Figure S5, SI). The pK_a values for Ru360′ were found to be 2.98(05) and 4.75(09) (Table 1). These values are lower than those previously reported (4.18 and 7.2).[34] Given the lack of experimental details in this previous report, we are unable to determine the source of the discrepancy between our values. We note that we have a rigorous setup and background in determining constants that describe aqueous equilibria,[46,47] and we therefore place a greater confidence in the values obtained in our lab. Based on these pK_a values, Ru360′ exists almost exclusively as the bishydroxo-capped species $[(HO)(NH_3)_4Ru(\mu\text{-}O)Ru(NH_3)_4(OH)]^{3+}$ at physiological pH of 7.4 (Figure S6 A, SI). As noted above, an important ramification of this conclusion is that this complex attains an overall +3 rather than +5 charge under these conditions.

For Ru265′, we found the pK_a values to be 5.14(02) and 7.00(11) (Table 1). These values are approximately 2 pK_a units higher than those of Ru360′. This result is consistent with the presence of the nitrido bridging ligand in Ru265, which has a higher *trans* influence than the oxo-bridge of Ru360′. Thus, a longer Ru-OH_2 interatomic distances are expected in Ru265, rendering these water ligands less acidic.[48] In contrast to Ru360′, Ru265′ exists as a mixture of the asymmetric hydroxo-aqua-capped $[(H_2O)(NH_3)_4Ru(\mu\text{-}N)Ru(NH_3)_4(OH)]^{4+}$ species and the symmetric hydroxo-capped species $[(HO)(NH_3)_4Ru(\mu\text{-}N)Ru(NH_3)_4(OH)]^{3+}$ in a ratio of approximately 28:72 at pH 7.4 (Figure S6 B, SI). Thus, Ru265′ forms complexes of both +4 and +3 charges at physiological pH.

Single crystals of Ru265′ were obtained by the vapor diffusion of ethanol into a dilute nitric acid solution of the compound over a time period of several weeks (Figure 2). Full structural refinement details as well as interatomic distances and angles are given in the SI (Tables S2–S3). The complex crystallizes as the fully protonated diaqua-capped form $[(H_2O)(NH_3)_4Ru(\mu\text{-}N)Ru(NH_3)_4(OH_2)]^{5+}$ with the +5 charge balanced by one chloride and four nitrate anions. The bridging nitrogen atom sits on a crystallographic inversion

 © 2020 Wiley-VCH Verlag GmbH & Co. KGaA, Weinheim

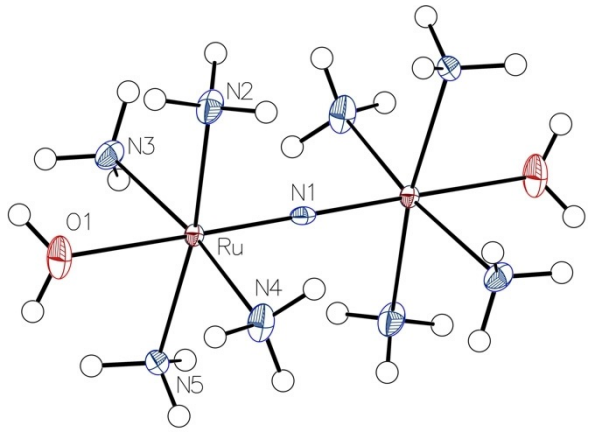

Figure 2. X-ray crystal structure of Ru265′. Outer sphere counterions and water molecules are omitted for clarity. Thermal ellipsoids are shown at the 50% probability level.

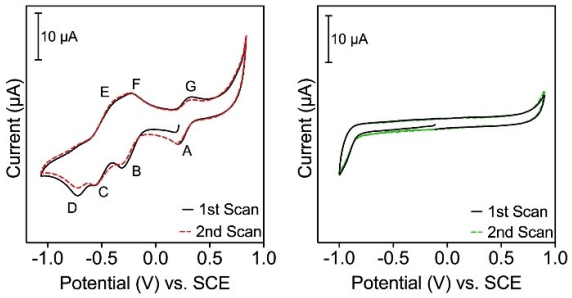

Figure 3. Cyclic voltammogram of Ru360′ (left) and Ru265′ (right) in 0.1 M ammonium formate (pH 7.4; 23 °C). Conditions: glassy carbon working electrode, Pt wire counter electrode, Ag/AgCl quasi-reference electrode and 0.1 Vs^{-1} scan rate. The first scan is represented by solid lines and the second scan by dashed lines. The first scan was initiated at the resting potentials of the solution (0.214 V and −0.112 V vs. SCE for Ru360′ and Ru265′ respectively) and swept initially to cathodic potentials. All potentials are referenced to the $[Ru(NH_3)_6]^{3+/2+}$ redox couple as an internal standard and are reported vs. SCE.

center, conferring the complex with rigorous C_i symmetry. As such, this complex features a perfectly linear (180°) Ru-N-Ru motif with the axial ammine ligands arranged in an eclipsed configuration. These features are similarly found in the crystal structure of chloride-capped Ru265 and aqua-capped Ru360′. The $Ru{-}N_{nitrido}$ distance (1.73871(15) Å) of Ru265′ is not significantly different from that of the chloride-capped Ru265 (1.7421(7) Å).[42] Consistent with the greater *trans* influence of the bridging nitrido ligand compared to the bridging oxo, the axial $Ru{-}OH_2$ distance in Ru265′ (2.140(2) Å) is significantly longer than that observed for Ru360′ (2.039(2) Å). The longer $Ru{-}OH_2$ distances of Ru265′ are in agreement with the higher pK_a values of this complex compared to Ru360′.

The redox activity of metal-based compounds can have a large role in mediating their biological effects and establishing their suitability as potential therapeutic agents.[49,50] Metal complexes that possess redox potentials within the range of −0.744 to +0.556 V (vs. SCE), which is the range of reduction potentials of most common biological reducing agents,[51] will likely undergo redox reactions in biological settings, which can either be leveraged to maximize an intended biological effect or can lead to compound deactivation by cellular reducing agents.[52–54] To determine the role of redox chemistry in mediating the biological activity of Ru265 and Ru360′, we investigated these complexes by cyclic voltammetry (CV) in pH 7.4 ammonium formate (Figure 3).

Ru360′ displays a reversible oxidation/reduction at 295 mV vs. SCE corresponding to the [III,IV]/[IV,IV] redox couple (Figure 3 A/G). Two quasi-reversible oxidation/reduction events, which are assigned to the [III,IV]/[III,III] (Figure 3 B/F) and [III,III]/[III,II] (Figure 3 C/E) redox couples, appear at −239 V and −475 V vs. SCE respectively (Table 1). Finally, an irreversible reduction, corresponding to the [III,II]/[II,II] reduction, appears at −0.740 mV vs. SCE (Figure 3 D, Table 1). By contrast, Ru265′ does not display any redox activity in 0.1 M ammonium formate within the range of −1 and 1 V vs. SCE (Figure 3, Table 1). We recently reported studies on a series of nitrido-bridged complexes of the general formula $[Ru_2(\mu\text{-}N)L_2Cl_5(DMF)]$ (L = 2,2′-bipyridine; 4,4′-dimethyl-2,2′-bipyridine; 4,4′-dimethoxy-2,2′-bipyridine).[41] These compounds display redox activity at potentials outside of the window of −1 to 1 V vs. SCE. Thus, it is likely that Ru265 possesses redox activity at more extreme potentials than those that could be afforded by the solvent window of water. The poor solubility of Ru265 in organic solvents precluded additional CV studies to directly probe this hypothesis. Based on the CV studies in aqueous solution, however, a key result is that Ru265, in contrast to Ru360′, is not expected to undergo redox reactions under biological conditions.

In our previous study, we have shown that Ru265 is taken up much more effectively than Ru360′ by both HeLa and HEK293 cells and localizes preferentially to the mitochondria.[42] To gain a more thorough understanding of the cellular uptake and localization of these complexes we employed synchrotron X-ray fluorescence (XRF) imaging. This technique can be used to generate element-specific maps of cells to determine the precise distribution of metals[55,56] and has previously been used to understand the cellular uptake and localization of Os, Ru, and Pt anticancer compounds.[57–60] For these experiments, we used HeLa cells grown on silicon nitride windows[61] that were treated with either 0 or 50 μM of Ru265 or Ru360′ for 3 hours at 37 °C prior to fixation with paraformaldehyde. Control cells were treated with equivalent volumes of media to determine background levels of Ru in untreated cells.

As shown in Figure 4, Figure 5, and Figures S7–S9 (SI), the XRF elemental mapping of cells treated with Ru265 show significantly increased cellular Ru levels compared to control cells, where the Ru level was below the detection limit (Figures 5 A, S7, S8, SI). Furthermore, the intracellular Ru content of these cells was substantially greater than those treated with Ru360′ (Figures 5 A, S8, S9, SI). These data confirm our prior graphite furnace atomic absorption spectroscopy (GFAAS) results that showed Ru265 to be taken up by cells more effectively than Ru360′.

In cells treated with Ru265, Ru was found primarily outside of the nuclear region, commonly localized around the nucleus but also spreading well into the cytoplasm (Figures 4,

 © 2020 Wiley-VCH Verlag GmbH & Co. KGaA, Weinheim

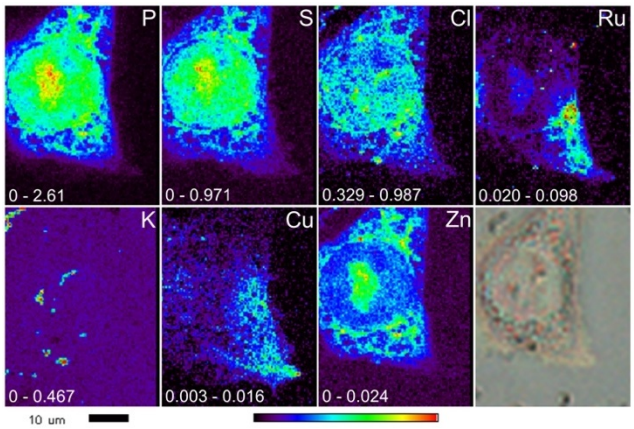

Figure 4. X-ray fluorescence elemental distribution maps and optical micrograph (bottom right) of a single HeLa cell treated with 50 μM Ru265 for 3 h at 37 °C. The maximal elemental area density (quantified from standards and expressed in $\mu g\,cm^{-2}$) is given at the bottom left of each map. The Ru map was collected with an incident energy of 22.7 keV, the other maps (P, S, Cl, K, Cu, Zn) were collected at 13.1 keV.

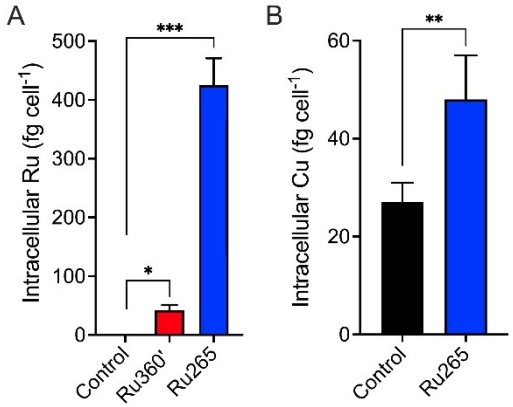

Figure 5. Average intracellular contents of (A) Ru and (B) Cu in HeLa cells quantified by analysis of XRF imaging data. Cell cultures were treated with either 0 or 50 μM of Ru360′ or Ru265 for 3 h at 37 °C. Error bars represent mean ± SD ($n = 4$–5; $*p < 0.05$, $**p < 0.005$, $***p < 0.001$).

S8, SI). Conversely, very limited Ru was detected in cells treated with Ru360′ and the observation of small, concentrated regions of Ru, sometimes completely separated from the cells, is indicative of the presence of extracellular precipitate that was not removed during the washing process (Figure S9, SI). The quantitation of Ru in Ru360′-treated cells (Figure 5 A) likely includes a spurious contribution from this extracellular precipitate, but we do note that detectable levels of Ru are present in these cells (Figures 5 A, S9, SI) and so some minor uptake was presumed to have occurred.

In all of the cells imaged, we observed localized extracellular distributions of K (Figures S7–S9, SI) and Ca (not shown), indicating the presence of detritus from sample preparation that was not removed by the washing steps. The presence of this extracellular precipitate combined with the use of a chemical fixative, which could perturb the distribution of such labile elements,[62] precludes reliable assessment of cellular K and Ca distribution by XRF imaging.

Interestingly, a change in cell morphology was noted in cells treated with 50 μM Ru265 compared to control, in both the optical micrographs and more notably in the elemental maps of the lighter elements and Zn (Figures 4, S7, and S8, SI). Ru265 treatment resulted in the formation of vesicles or vacuoles in the cytoplasm with much lower levels of all measured elements, but these observations were not particularly associated with the observed distribution of Ru. Additionally, these morphological changes are not observed when performing imaging studies on live cells treated with the complex. The exact implications of this phenomenon is not evident from the data at hand and merits further study to determine the potential causes of this result.

Statistical analysis of elemental contents in cells treated with Ru265, determined by XRF imaging, revealed significant increases in cellular P and Cu levels, but no significant changes in cellular S, Cl, or Zn (Figure 5 B, S10). The increase in cellular Cu levels in cells treated with Ru265 was an unexpected result. Similar results have been observed in cells exposed to selenite, where the cells display increased Cu levels in addition to stimulation of antioxidant response and expression of superoxide dismutase 1 (SOD1).[63,64] The apparently lack of redox activity of Ru265, however, indicates that a different cellular response is at play. It was recently reported that modulation of cellular Ca^{2+} levels induced dynamic copper redistribution in neuronal cells.[65] It is feasible that increased cytosolic Ca^{2+} levels, a direct result of MCU inhibition by Ru265, could alter cellular copper pools, leading to the observed increase. This potential link between Ru265 treatment, Ca^{2+} concentration, and cellular Cu levels is interesting and merits further investigation.

Collectively, our previous GFAAS and current XRF data both verify that Ru265 exhibits significantly enhanced cellular accumulation compared to Ru360′. A key question that remains, however, is why Ru265 is more amenable to cell uptake than Ru360′. To address this question, we initiated an investigation on the mechanism of cellular uptake of these compounds. By understanding the cellular uptake mechanism, we reasoned that we could rationalize the disparate uptake efficiencies of these compounds.

We first investigated whether Ru265, Ru265′, and Ru360′ enter cells in an energy-dependent manner. HeLa cells were treated with 50 μM of the Ru complex as the chloride salt and incubated at 37 or 4 °C for 3 hours before the cells were washed, harvested, and lysed. The cellular ruthenium content was measured by GFAAS and normalized to the cellular protein levels, which were determined using the bicinchoninic acid (BCA) assay. A cell viability assay confirmed that the cells remained viable during incubation at low temperatures (Figure S11, SI). As shown in Figure 6, the cellular uptake of Ru265 and Ru265′ is nearly identical under all conditions screened. This result is consistent with our aquation studies that demonstrate that Ru265 is rapidly transformed to Ru265′ within minutes under physiological conditions. Thus, it is unlikely that this ligand substitution process gates the cell uptake of this compound. Additionally, consistent with prior

 © 2020 Wiley-VCH Verlag GmbH & Co. KGaA, Weinheim

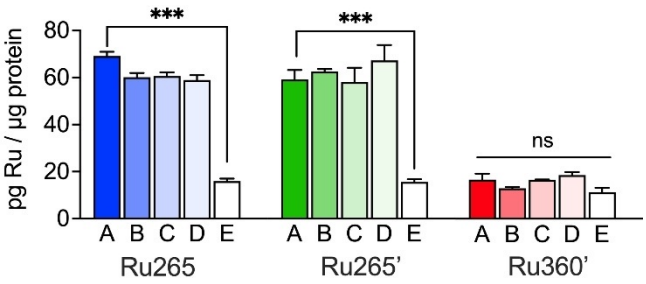

Figure 6. Cellular uptake of Ru265 (blue), Ru265′ (green), and Ru360′ (red) in HeLa cells (50 µM, 3 h dose) under different incubation conditions. (A) 0.5% DMSO; (B) 4 °C; (C) 50 mM 2-deoxy-D-glucose and 5 µM Oligomycin A; (D) 200 µM $CuSO_4$; (E) 1 mM Procainamide. Ruthenium concentration was quantified using GFAAS and normalized to protein content as measured by the BCA assay. Error bars represent mean ± SD ($n = 3$–6; *ns* = not significant, ***$p < 0.001$).

studies, Ru360′ is generally taken up to a significantly smaller extent than Ru265.

The temperature-dependent data show that there are no differences in cellular uptake of the complexes at 37 °C and 4 °C (Figure 6 A,B). This result suggests that cellular uptake of Ru265 occurs in an energy-independent manner. To account for the fact that incubation at low temperature can alter the fluidity of the cell membrane[66] and may affect the cellular accumulation of the complexes, we also monitored the effect of 2-deoxyglucose (50 mM) and oligomycin A (5 µM), which inhibit glycolysis and oxidative phosphorylation, respectively,[67] on the uptake of the Ru compounds. These reagents, which deplete cellular ATP, do not affect the uptake of any of the complexes, providing further confirmation that this compound enters cells in an energy-independent manner (Figure 6 C).

Given the high cationic charge of Ru265, Ru265′, and Ru360′, it is unlikely that they cross the cell membrane by passive diffusion. Thus, we investigated the role of energy-independent transporter proteins in the uptake of these complexes. Coincubation with 200 µM $CuSO_4$, which will saturate the copper transporter CTR1, does not alter the cellular accumulation of any of the complexes (Figure 6 D), suggesting that they are not being taken up by this pathway. This result is in contrast to that for the platinum-based anticancer drugs, whose uptake is correlated to CTR1 expression levels.[68,69] Incubation with the organic cation transporter (OCT) inhibitor procainamide significantly reduced the cellular uptake levels of Ru265 and Ru265′, but not Ru360′ (Figure 6 E). The organic cation transporters OCT1, OCT2, and OCT3 are primarily responsible for the transport of signaling molecules and metabolites such as dopamine, serotonin, and choline. However, these transporters have recently been shown to mediate the uptake of several cationic monofunctional platinum(II) anticancer complexes,[69–74] suggesting that they may have a more general affinity for coordination complexes.

Because procainamide inhibits all three OCTs, we carried out further studies to identify the specific OCT responsible for mediating Ru265 uptake. HEK293 cells transfected with the vectors to overexpress human OCT1, OCT2, and OCT3 were used for these studies. Cells transfected with the empty vector (EV) served as controls. The levels of overexpression were measured with real-time quantitative polymerase chain reaction (RT-qPCR) techniques.[75] The primers used in the qPCR assay are shown in Table S4 (SI). All transfected cell lines display OCT expression levels at least 500 times greater than the control EV cells (Figure S12, SI).

Cells overexpressing OCT1 and OCT2 did not exhibit increased uptake of Ru265 or Ru360′ compared to the EV cells, and coincubation with the OCT1-specific inhibitor ketoconazole (10 µM) or OCT2-specific inhibitor cimetidine (1.5 mM) had no effect on the accumulation of the complexes (Figure 7). When the uptake experiments were performed in cells expressing OCT3, however, the cellular ruthenium concentration of cells treated with Ru265 was over four times greater than that found in the EV cells. Furthermore, coincubation with the OCT3-specific inhibitor corticosterone (200 µM) ablates the uptake of Ru265 in OCT3 cells. A similar degree of enhancement of compound uptake was observed for the drug metformin, which is a known substrate for OCT1. HEK293 cells overexpressing OCT1 display an approximately five-fold increase in metformin accumulation compared to

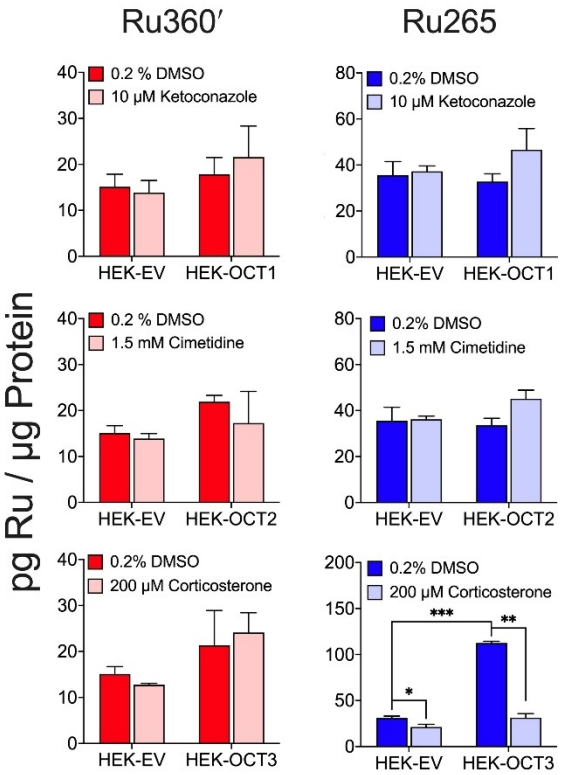

Figure 7. Cellular uptake of Ru360′ (left, red) or Ru265 (right, blue) in transfected HEK293 cells (50 µM, 3 h dose) in the presence or absence of inhibitors. Top: OCT1-expressing (HEK-OCT1) and empty vector (HEK-EV) treated cells were treated with Ru360′ or Ru265 in the presence or absence of 10 µM ketoconazole. Center: OCT2-expressing (HEK-OCT2) and HEK-EV cells were treated with Ru360′ or Ru265 in the presence or absence of 1.5 mM cimetidine. Bottom: OCT3-expressing (HEK-OCT3) and HEK-EV cells were treated with Ru360′ or Ru265 in the presence or absence of 200 µM corticosterone. Error bars represent mean ± SD ($n = 4$–6; *$p < 0.05$; **$p < 0.01$, ***$p < 0.001$).

 © 2020 Wiley-VCH Verlag GmbH & Co. KGaA, Weinheim

wild-type cells that was sensitive to inhibition by quinidine, an OCT1 inhibitor.[76] The magnitude of this increase in compound accumulation is comparable to what we observed for Ru265 in cells overexpressing OCT3. Ru360′ did not show a similar increase in uptake, suggesting that this complex is not transported by OCT3 (Figure 7).

On the basis of these results, our data highlights the role of OCT3 in the cellular accumulation of Ru265 and may provide an explanation for its increased cell permeability compared to Ru360′. In contrast to OCT1 and OCT2, which are most highly expressed in the liver and kidney, respectively,[77] OCT3 is more widely distributed throughout the body with highest expression found in the heart, skeletal muscle, placenta, and brain.[77–79] The tissue distribution profile of OCT3 suggests that Ru265 may localize to these tissues. Thus, Ru265 is expected to be a highly valuable tool for studying the role of MCU-mediated Ca^{2+} regulation in diseases related to the heart, brain, and skeletal muscle such as ischemic stroke, neurodegeneration, and cardiovascular disease in vivo.[80–82]

The studies above clearly demonstrate that Ru265 is taken up more efficiently than Ru360′, despite being structurally similar. When performing our cellular uptake studies, we were surprised to find that the cellular uptake of Ru360′ was sensitive to the presence of fetal bovine serum (FBS). When cells were treated with Ru360′ in the absence of FBS, the cellular accumulation of this compound was significantly higher than when it was administered in media supplemented with 10% FBS (Figure 8). In contrast, cells treated with Ru265 showed no FBS-dependent changes in Ru accumulation. Like Ru360′, several Ti^{IV} complexes show a decreased cellular uptake in the presence of FBS. In this case, this result has been attributed to tight binding of the complexes to biomolecules, such as albumin, which limits their release in cells.[83–86]

To determine if the decreased uptake of Ru360′ in the presence of FBS is due to protein binding like the Ti^{IV} complexes, we incubated this complex (100 μM) in cell culture media containing 0 or 10% FBS at 37 °C and analyzed these solutions by GFAAS after separating the high and low molecular weight fractions. More specifically, aliquots of the solution were removed at different time points and then centrifuged through a 3 kDa molecular weight cutoff filter.

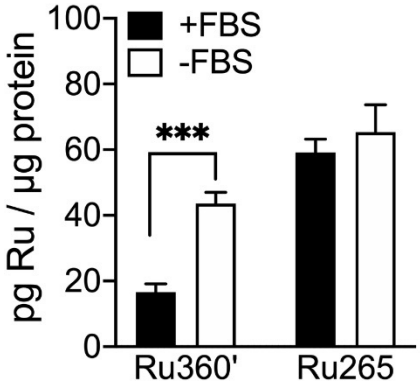

Figure 8. Cellular uptake of Ru360′ and Ru265 in the presence (black) or absence (white) of FBS (50 μM, 3 h dose). Data represent mean ± SD (***$p < 0.001$; $n = 4$–6).

The amount of Ru in the filtrate, measured by GFAAS, corresponds to the quantity of Ru360′ that is not bound to proteins including albumin, which has a MW greater than 3 kDa. Only a minor (< 11%) decrease in the amount of Ru in the small MW fraction was observed over an 8 hour period (Figure S13, SI), indicating that Ru360′ does bind to high MW proteins with appreciable affinity. Because the cellular uptake experiments in the presence and absence of FBS (Figure 8) were carried out after a 3 hour incubation period, the minor extent of Ru360′ binding to proteins after a significantly longer 8 hour incubation is unlikely to be a contributing factor to its decreased uptake in the presence of FBS.

The physical characterization data of Ru360′ and Ru265 discussed above shows that a major difference between these complexes arises within their redox activities. In contrast to Ru360′, Ru265 shows no redox events within biologically accessible potentials (Figure 3 and Table 1). As such, we explored the role of biological reduction in the MCU inhibition induced by these compounds. As the cyclic voltammograms in Figure 3 show, the reductions of Ru360′ are irreversible. The irreversible nature of these redox events may be a consequence of rapid chemical decomposition of this compound rapidly after reduction.[34,87] Supporting this conclusion, Ru360′ loses its ability to inhibit the MCU when incubated with biologically relevant reducing agents. Solutions of Ru360′ and Ru265 (10 μM) were treated with glutathione (GSH; 2 mM), sodium ascorbate (Asc; 250 μM), sodium sulfite (250 μM), or sodium dithionite (250 μM) and incubated at 37 °C in pH 7.4 MOPS buffer (50 mM) for 2, 12, and 24 h prior to assessing their abilities to inhibit MCU-mediated Ca^{2+} uptake in permeabilized HeLa cells. Control cells were treated with the reductant alone to control for their potential effect on MCU activity.

Incubation of Ru360′ with GSH and Asc induced a time-dependent loss in MCU-inhibitory activity, with full loss of inhibition observed after 24 h. Incubation with the stronger reductants SO_3^{2-} and $S_2O_4^{2-}$ gives rise to near complete loss of inhibitory activity after just 2 hours (Figure S14, SI). Thus, these results clearly show that reduction of Ru360′ leads to products that are inactive for MCU inhibition. When we subjected Ru265 to the same conditions with the same reducing agents, no loss of MCU-inhibitory activity is observed. This result is consistent with the lack of redox activity observed via our electrochemical studies. Because FBS is known to contain small-molecule reductants and antioxidant enzymes, we hypothesized that Ru360′ could be reduced in culture media containing this supplement. Furthermore, metal complexes of Au, Pt, and Ru have previously been shown to be reduced by such biomolecules.[88–90] To test this hypothesis, we incubated Ru360′ in MOPS buffer containing 10% FBS for 3 hours at 37 °C, prior to its administration to permeabilized HeLa cells. As shown in Figure 8A, the mitochondrial calcium uptake inhibitory properties of this compound are significantly diminished after exposure to FBS (Figure 9A). In contrast, when Ru265 was preincubated with FBS under the same conditions, no loss of MCU-inhibitory activity is observed (Figure 9B). Thus, Ru360′, but not Ru265, is most likely reduced by components within FBS, leading to its deactivation. Based on the cell

 © 2020 Wiley-VCH Verlag GmbH & Co. KGaA, Weinheim

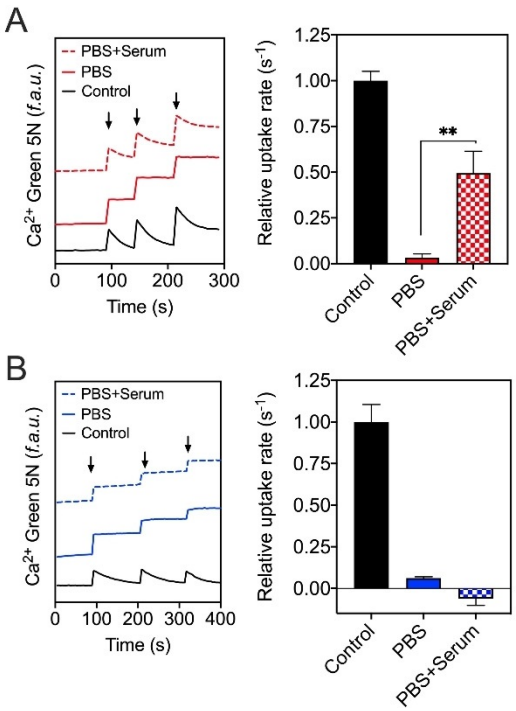

Figure 9. Changes in extramitochondrial calcium levels in permeabilized HeLa cells treated with 500 nM (A) Ru360′ and (B) Ru265 that had been preincubated in PBS containing 0 or 10% FBS for 3 h at 37 °C. Bar graphs represent quantification of the mitochondrial Ca^{2+} accumulation rate as a function of the decrease in cytosolic Ca^{2+} (see SI for details). Arrows indicate time of Ca^{2+} addition. Error bars represent mean relative Ca^{2+} uptake rate ± SD (**$p < 0.01$; $n = 3$–4).

uptake data in the presence and absence of FBS (Figure 8), we further hypothesize that the extracellular reduction of Ru360′ gives rise to Ru compounds that are poorly cell permeable and not efficient substrates for OCT3. Therefore, the poor redox stability of Ru360′ in biologically relevant conditions provides a likely explanation for its inability to cross the cell membrane and inhibit the MCU in non-permeabilized cells. (Figures 8 and S10).

Conclusion

Although Ru360 is a widely used and selective inhibitor for the MCU, its widespread applicability is diminished by its low cell permeability and its inability to inhibit mitochondrial calcium uptake in intact cells. These challenges prevent its use as a potential therapeutic drug or as a tool to study the dynamics of mitochondrial Ca^{2+} uptake. Surprisingly, there have been no studies focused on understanding why Ru360 is ineffective in intact biological systems. We have recently reported on the synthesis and characterization of Ru265 as a functional analogue of Ru360′. This compound is significantly more cell permeable than Ru360′ and is highly selective for MCU inhibition. A question that we sought to address is why Ru265 is more effective in intact cell systems than Ru360′, despite their similar structures.

Although these compounds are structurally similar, Ru265 and Ru360′ exhibit slightly different physical properties (Table 1). The most striking difference between the complexes arises from a comparison of their redox activity. Upon reduction by biological reducing agents, Ru360′ loses the ability to inhibit the MCU. Ru265 does not display any redox activity within the biological window and as such does not lose its inhibitory activity even after incubation with 25 equivalents of $S_2O_4^-$ for 24 h at 37 °C. This redox activity may explain why Ru360′ is unable to reliably cross the cell membrane and inhibit the MCU in physiological environments.

Our efforts to understand the mechanism of cellular accumulation of Ru265 and Ru360′ revealed the surprising role of the organic cation transporter OCT3 in the uptake of these complexes. To the best of our knowledge, no other transition metal complexes have been previously reported to be substrates of OCT3. It is known that relatively minor structural changes can drastically affect the biological activity of metallodrugs.[91–93] It is surprising, however, that the alteration of the bridging atom alone in these complexes is enough to change the affinity of these complexes for OCT3.

A potential explanation for the increased uptake of Ru265 through OCT3 compared to Ru360′ could be their difference in redox activity. We demonstrated that Ru360′ loses its ability to inhibit the MCU when the complex is incubated in pH 7.4 MOPS buffer in the presence of serum. We further showed that the inhibitory properties of Ru360′ are ablated in the presence of biological reducing agents. On the basis of these results, it is feasible that Ru360′ is reduced extracellularly by biological antioxidants that are present in serum. This reduced form of the complex may undergo chemical decomposition or be otherwise deactivated such that it is not able to be transported across the cell membrane by OCT3.

The results reported here provide some basis for understanding the biological activity of ruthenium-based MCU inhibitors. Knowledge of how the physical properties of Ru265 and Ru360′ relate to the mechanism of cellular uptake can now be applied to the design of future MCU inhibitors for therapeutic applications.

Acknowledgements

This work was supported by the National Science Foundation (NSF-GRFP for J. J. Woods; award no. DGE-1650441 and NSF Career Award for J. J. Wilson; award no. CHE-1750295) and the American Heart Association (AHA Predoctoral Fellowship for J. J. Woods; award no. 20PRE35120390). This study made use of the Cornell NMR facility, which is supported in part by the NSF (CHE-1531632). The research additionally made use of resources at the Advanced Photon Source, a U.S. Department of Energy (DOE) Office of Science User Facility operated for the DOE Office of Sciences by Argonne National Laboratory under contract No. DE-AC02-06CH11357. Travel funding for H. H. Harris and J. H. Lovett to perform experiments at the Advanced Photon Source was provided by the International Synchrotron Access Program (ISAP) managed by the Australian

 © 2020 Wiley-VCH Verlag GmbH & Co. KGaA, Weinheim

Synchrotron, part of ANSTO, funded by the Australian Government. The authors would like to thank Professor Kathleen M. Giacomini (UCSF) for supplying the HEK293 cells transfected to express OCT1-3. Huan-Cheih Chien and Sook Wah Yee are thanked for discussions on culturing and cellular uptake protocols for the transfected cell lines. Robert Swanda and Dr. Nikki Thiele are thanked for assistance with qPCR and spectrophotometric titrations, respectively.

Conflict of interest

The authors declare no conflict of interest.

Keywords: bioinorganic chemistry · mitochondrial calcium uniporter · organic cation transporter · ruthenium · X-ray fluorescence imaging

How to cite: *Angew. Chem. Int. Ed.* **2020**, *59*, 6482 – 6491
Angew. Chem. **2020**, *132*, 6544 – 6553

[1] D. E. Clapham, *Cell* **2007**, *131*, 1047 – 1058.
[2] D. De Stefani, A. Raffaello, E. Teardo, I. Szabò, R. Rizzuto, *Nature* **2011**, *476*, 336 – 340.
[3] C. Fan, M. Fan, B. J. Orlando, N. M. Fastman, J. Zhang, Y. Xu, M. G. Chambers, X. Xu, K. Perry, M. Liao, L. Feng, *Nature* **2018**, *559*, 575 – 579.
[4] R. Baradaran, C. Wang, A. F. Siliciano, S. B. Long, *Nature* **2018**, *559*, 580 – 584.
[5] N. X. Nguyen, J. P. Armache, C. Lee, Y. Yang, W. Zeng, V. K. Mootha, Y. Cheng, X. Bai, Y. Jiang, *Nature* **2018**, *559*, 570 – 574.
[6] J. Yoo, M. Wu, Y. Yin, M. A. Herzik, G. C. Lander, S.-Y. Lee, *Science* **2018**, *361*, 506 – 511.
[7] Y. Lee, C. K. Min, T. G. Kim, H. K. Song, Y. Lim, D. Kim, K. Shin, M. Kang, J. Y. Kang, H.-S. Youn, et al., *EMBO Rep.* **2015**, *16*, 1318 – 1333.
[8] S. K. Lee, S. Shanmughapriya, M. C. Y. Mok, Z. Dong, D. Tomar, E. Carvalho, S. Rajan, M. S. Junop, M. Madesh, P. B. Stathopulos, *Cell Chem. Biol.* **2016**, *23*, 1157 – 1169.
[9] J. Q. Kwong, *J. Physiol.* **2017**, *595*, 3743 – 3751.
[10] E. J. Griffiths, *J. Mol. Cell. Cardiol.* **2009**, *46*, 789 – 803.
[11] D. G. Nicholls, *Neurochem. Int.* **2017**, *109*, 5 – 12.
[12] E. Pchitskaya, E. Popugaeva, I. Bezprozvanny, *Cell Calcium* **2018**, *70*, 87 – 94.
[13] A. Vultur, C. S. Gibhardt, H. Stanisz, I. Bogeski, *Pflügers Arch. J. Physiol.* **2018**, *470*, 1149 – 1163.
[14] C. Giorgi, C. Agnoletto, A. Bononi, M. Bonora, E. De Marchi, S. Marchi, S. Missiroli, S. Patergnani, F. Poletti, A. Rimessi, J. M. Suski, M. R. Wieckowski, P. Pinton, *Mitochondrion* **2012**, *12*, 77 – 85.
[15] E. Penna, J. Espino, D. De Stefani, R. Rizzuto, *Cell Calcium* **2018**, *69*, 73 – 80.
[16] W. Wang, G. Karamanlidis, R. Tian, *Sci. Transl. Med.* **2016**, *8*, 326rv3.
[17] C. Mammucari, G. Gherardi, R. Rizzuto, *Front. Oncol.* **2017**, *7*, 139.
[18] N. Nemani, S. Shanmughapriya, M. Madesh, *Cell Calcium* **2018**, *74*, 86 – 93.
[19] J. J. Woods, J. J. Wilson, *Curr. Opin. Chem. Biol.* **2020**, *55*, 9 – 18.
[20] J. Santo-Domingo, L. Vay, E. Hernández-Sanmiguel, C. D. Lobatón, A. Moreno, M. Montero, J. Alvarez, *Br. J. Pharmacol.* **2007**, *151*, 647 – 654.
[21] D. M. Arduino, J. Wettmarshausen, H. Vais, P. Navas-Navarro, Y. Cheng, A. Leimpek, Z. Ma, A. Delrio-Lorenzo, A. Giordano, C. Garcia-Perez, G. Médard, B. Kuster, J. García-Sancho, D. Mokranjac, J. K. Foskett, M. T. Alonso, F. Perocchi, *Mol. Cell* **2017**, *67*, 711 – 723.
[22] N. Kon, M. Murakoshi, A. Isobe, K. Kagechika, N. Miyoshi, T. Nagayama, *Cell Death Discovery* **2017**, *3*, 17045.
[23] A. Degterev, A. Linkermann, *Cell. Mol. Sci.* **2016**, *73*, 2251 – 2267.
[24] V. T. Thu, H. K. Kim, L. T. Long, S. R. Lee, T. M. Hanh, T. H. Ko, H. J. Heo, N. Kim, S. H. Kim, K. S. Ko, B. D. Rhee, J. Han, *Cardiovasc. Res.* **2012**, *94*, 342 – 350.
[25] K. J. Kelly, T. A. Sutton, N. Weathered, N. Ray, E. J. Caldwell, Z. Plotkin, P. C. Dagher, *Am. J. Physiol.* **2004**, *287*, F760 – F766.
[26] H. J. Kim, S. Y. Koo, B.-H. Ahn, O. Park, D. H. Park, D. O. Seo, J. H. Won, H. J. Yim, H.-S. Kwak, H. S. Park, C. W. Chung, Y. L. Oh, S. H. Kim, *Arch. Pharmacal Res.* **2010**, *33*, 1813 – 1823.
[27] Y. N. Antonenko, T. I. Rokitskaya, A. J. L. Cooper, B. F. Krasnikov, *J. Bioenerg. Biomembr.* **2010**, *42*, 151 – 163.
[28] T. P. Theruvath, Z. Zhong, P. Pediaditakis, V. K. Ramshesh, R. T. Currin, A. Tikunov, E. Holmuhamedov, J. J. Lemasters, *Hepatology* **2008**, *47*, 236 – 246.
[29] P. J. Smith, S. A. Morgan, M. E. Fox, J. V. Watson, *Biochem. Pharmacol.* **1990**, *40*, 2069 – 2078.
[30] M. P. Boland, K. A. Fitzgerald, L. A. J. O'Neill, *J. Biol. Chem.* **2000**, *275*, 25231 – 25238.
[31] R. Payne, C. Li, E. Fernandez-Garcia, H. Vais, K. Foskett, *Biophys. J.* **2019**, *116*, 270a.
[32] H. Nägele, M. A. Castel, O. Deutsch, F. M. Wagner, H. Reichenspurner, *J. Heart Lung Transplant.* **2004**, *23*, 641 – 643.
[33] W.-L. Ying, J. Emerson, M. J. Clarke, D. Rao Sanadi, *Biochemistry* **1991**, *30*, 4949 – 4952.
[34] J. Emerson, M. J. Clarke, W. L. Ying, D. R. Sanadi, *J. Am. Chem. Soc.* **1993**, *115*, 11799 – 11805.
[35] M. A. Matlib, Z. Zhou, S. Knight, S. Ahmed, K. M. Choi, J. Krause-Bauer, R. Phillips, R. Altschuld, Y. Katsube, N. Sperelakis, D. M. Bers, *J. Biol. Chem.* **1998**, *273*, 10223 – 10231.
[36] G. D. J. García-Rivas, A. Guerrero-Hernández, G. Guerrero-Serna, J. S. Rodríguez-Zavala, C. Zazueta, *FEBS J.* **2005**, *272*, 3477 – 3488.
[37] E. J. Griffiths, *FEBS Lett.* **2000**, *486*, 257 – 260.
[38] G. J. García-Rivas, K. Carvajal, F. Correa, C. Zazueta, *Br. J. Pharmacol.* **2006**, *149*, 829 – 837.
[39] S. R. Nathan, N. W. Pino, D. M. Arduino, F. Perocchi, S. N. MacMillan, J. J. Wilson, *Inorg. Chem.* **2017**, *56*, 3123 – 3126.
[40] S. R. Nathan, J. J. Wilson, *J. Vis. Exp.* **2017**, *128*, e56527.
[41] J. Urgiles, S. R. Nathan, S. N. MacMillan, J. J. Wilson, *Dalton Trans.* **2017**, *46*, 14256 – 14263.
[42] J. J. Woods, N. Nemani, S. Shanmughapriya, A. Kumar, M. Zhang, S. R. Nathan, M. Thomas, E. Carvalho, K. Ramachandran, S. Srikantan, P. B. Stathopulos, J. J. Wilson, M. Madesh, *ACS Cent. Sci.* **2019**, *5*, 153 – 166.
[43] D. Chaudhuri, D. J. Artiga, S. A. Abiria, D. E. Clapham, *Proc. Natl. Acad. Sci. USA* **2016**, *113*, E1872 – E1880.
[44] K. M. Broekemeier, R. J. Krebsbach, D. R. Pfeiffer, *Mol. Cell. Biochem.* **1994**, *139*, 33 – 40.
[45] D. C. Crans, K. A. Woll, K. Prusinskas, M. D. Johnson, E. Norkus, *Inorg. Chem.* **2013**, *52*, 12262 – 12275.
[46] N. A. Thiele, S. N. MacMillan, J. J. Wilson, *J. Am. Chem. Soc.* **2018**, *140*, 17071 – 17078.
[47] N. A. Thiele, J. J. Woods, J. J. Wilson, *Inorg. Chem.* **2019**, *58*, 10483 – 10500.
[48] M. J. Cleare, W. P. Griffith, *J. Chem. Soc. A* **1970**, 1117 – 1125.
[49] I. Romero-Canelón, P. J. Sadler, *Inorg. Chem.* **2013**, *52*, 12276 – 12291.
[50] C. S. Allardyce, P. J. Dyson, *Dalton Trans.* **2016**, *45*, 3201 – 3209.

 © 2020 Wiley-VCH Verlag GmbH & Co. KGaA, Weinheim

[51] D. C. Harris, *Quantitative Chemical Analysis*, W. H. Freeman And Company, New York, **1998**.
[52] H. Petzold, P. J. Sadler, *Chem. Commun.* **2008**, 4413 – 4415.
[53] A. De Luca, L. J. Parker, W. H. Ang, C. Rodolfo, V. Gabbarini, N. C. Hancock, F. Palone, A. P. Mazzetti, L. Menin, C. J. Morton, M. W. Parker, M. Lo Bello, P. J. Dyson, *Proc. Natl. Acad. Sci. USA* **2019**, *116*, 13943 – 13951.
[54] P. Zhang, P. J. Sadler, *Eur. J. Inorg. Chem.* **2017**, 1541 – 1548.
[55] A. A. Hummer, A. Rompel, *Metallomics* **2013**, *5*, 597 – 614.
[56] M. J. Pushie, I. J. Pickering, M. Korbas, M. J. Hackett, G. N. George, *Chem. Rev.* **2014**, *114*, 8499 – 8541.
[57] C. Sanchez-Cano, I. Romero-Canelón, Y. Yang, I. J. Hands-Portman, S. Bohic, P. Cloetens, P. J. Sadler, *Chem. Eur. J.* **2017**, *23*, 2512 – 2516.
[58] J. B. Aitken, S. Antony, C. M. Weekley, B. Lai, L. Spiccia, H. H. Harris, *Metallomics* **2012**, *4*, 1051 – 1056.
[59] M. D. Hall, C. T. Dillon, M. Zhang, P. Beale, Z. Cai, B. Lai, A. P. J. Stampfl, T. W. Hambley, *J. Biol. Inorg. Chem.* **2003**, *8*, 726 – 732.
[60] P. Ilinski, B. Lai, Z. Cai, W. Yun, D. Legnini, T. Talarico, M. Cholewa, L. K. Webster, G. B. Deacon, S. Rainone, D. R. Phillips, A. P. J. Stampfl, *Cancer Res.* **2003**, *63*, 1776 – 1779.
[61] E. A. Carter, B. S. Rayner, A. I. McLeod, L. E. Wu, C. P. Marshall, A. Levina, J. B. Aitken, P. K. Witting, B. Lai, Z. Cai, S. Vogt, Y.-C. Lee, C.-I. Chen, M. J. Tobin, H. H. Harris, P. A. Lay, *Mol. Biosyst.* **2010**, *6*, 1316.
[62] M. J. Hackett, J. A. McQuillan, F. El-Assaad, J. B. Aitken, A. Levina, D. D. Cohen, R. Siegele, E. A. Carter, G. E. Grau, N. H. Hunt, P. A. Lay, *Analyst* **2011**, *136*, 2941 – 2952.
[63] C. M. Weekley, J. B. Aitken, S. Vogt, L. A. Finney, D. J. Paterson, M. D. De Jonge, D. L. Howard, P. K. Witting, I. F. Musgrave, H. H. Harris, *J. Am. Chem. Soc.* **2011**, *133*, 18272 – 18279.
[64] C. M. Weekley, G. Jeong, M. E. Tierney, F. Hossain, A. M. Maw, A. Shanu, H. H. Harris, P. K. Witting, *J. Biol. Inorg. Chem.* **2014**, *19*, 813 – 828.
[65] S. C. Dodani, D. W. Domaille, C. I. Nam, E. W. Miller, L. A. Finney, S. Vogt, C. J. Chang, *Proc. Natl. Acad. Sci. USA* **2011**, *108*, 5980 – 5985.
[66] R. B. Gennis, *Biomembranes: Molecular Structure and Function*, Springer, New York, **1989**.
[67] T. TeSlaa, M. A. Teitell, *Methods Enzymol.* **2014**, *542*, 91 – 114.
[68] S. S. More, O. Akil, A. G. Ianculescu, E. G. Geier, L. R. Lustig, K. M. Giacomini, *J. Neurosci.* **2010**, *30*, 9500 – 9509.
[69] I. Buß, A. Hamacher, N. Sarin, M. U. Kassack, G. V. Kalayda, *Metallomics* **2018**, *10*, 414 – 425.
[70] S. Zhang, K. S. Lovejoy, J. E. Shima, L. L. Lagpacan, Y. Shu, A. Lapuk, Y. Chen, T. Komori, J. W. Gray, X. Chen, S. J. Lippard, K. M. Giacomini, *Cancer Res.* **2006**, *66*, 8847 – 8857.
[71] H. Burger, A. Zoumaro-Djayoon, A. W. M. Boersma, J. Helleman, E. M. J. J. Berns, R. H. J. Mathijssen, W. J. Loos, E. A. C. Wiemer, *Br. J. Pharmacol.* **2010**, *159*, 898 – 908.
[72] S. S. More, S. Li, S. W. Yee, L. Chen, Z. Xu, D. M. Jablons, K. M. Giacomini, *Mol. Cancer Ther.* **2010**, *9*, 1058 – 1069.
[73] A. Hucke, G. Y. Park, O. B. Bauer, G. Beyer, C. Köppen, D. Zeeh, C. A. Wehe, M. Sperling, R. Schröter, M. Kantauskaitè, Y. Hagos, U. Karst, S. J. Lippard, G. Ciarimboli, *Front. Chem.* **2018**, *6*, 180.
[74] K. S. Lovejoy, R. C. Todd, S. Zhang, M. S. McCormick, J. A. D′Aquino, J. T. Reardon, A. Sancar, K. M. Giacomini, S. J. Lippard, *Proc. Natl. Acad. Sci. USA* **2008**, *105*, 8902 – 8907.
[75] K. J. Livak, T. D. Schmittgen, *Methods* **2001**, *25*, 402 – 408.
[76] Y. Shu, C. M. Brett, K. M. Giacomini, S. A. Sheardown, C. Brown, R. P. Owen, S. Zhang, R. A. Castro, A. G. Ianculescu, L. Yue, J. C. Lo, E. G. Burchard, *J. Clin. Invest.* **2007**, *117*, 1422 – 1431.
[77] H. Koepsell, K. Lips, C. Volk, *Pharm. Res.* **2007**, *24*, 1227 – 1251.
[78] X. Wu, R. Kekuda, W. Huang, Y.-J. Fei, F. H. Leibach, J. Chen, S. J. Conway, V. Ganapathy, *J. Biol. Chem.* **1998**, *273*, 32776 – 32786.
[79] V. Vialou, A. Amphoux, R. Zwart, B. Giros, S. Gautron, *J. Neurosci.* **2004**, *24*, 2846 – 2851.
[80] Y. Liao, Y. Dong, J. Cheng, *Int. J. Mol. Sci.* **2017**, *18*, 248.
[81] T. S. Luongo, J. P. Lambert, A. Yuan, X. Zhang, P. Gross, J. Song, S. Shanmughapriya, E. Gao, M. Jain, S. R. Houser, W. J. Koch, J. Y. Cheung, M. Madesh, J. W. Elrod, *Cell Rep.* **2015**, *12*, 23 – 34.
[82] T. Kalogeris, C. P. Baines, M. Krenz, R. J. Korthuis, *Int. Rev. Cell Mol. Biol.* **2012**, *298*, 229 – 317.
[83] J. Schur, C. M. Manna, A. Deally, R. W. Köster, M. Tacke, E. Y. Tshuva, I. Ott, *Chem. Commun.* **2013**, *49*, 4785 – 4787.
[84] T. B. Parks, Y. M. Cruz, A. D. Tinoco, *Inorg. Chem.* **2014**, *53*, 1743 – 1749.
[85] A. Vessières, M. A. Plamont, C. Cabestaing, J. Claffey, S. Dieckmann, M. Hogan, H. Müller-Bunz, K. Strohfeldt, M. Tacke, *J. Organomet. Chem.* **2009**, *694*, 874 – 879.
[86] M. Cini, T. D. Bradshaw, S. Woodward, *Chem. Soc. Rev.* **2017**, *46*, 1040 – 1051.
[87] A. L. Gushchin, Y. A. Laricheva, P. A. Abramov, M. N. Sokolov, P. A. Abramov, *Inorg. Chem. Commun.* **2018**, *95*, 163 – 166.
[88] A. Casini, M. A. Cinellu, G. Minghetti, C. Gabbiani, M. Coronnello, E. Mini, L. Messori, *J. Med. Chem.* **2006**, *49*, 5524 – 5531.
[89] J. Christodoulou, P. J. Sadler, A. Tucker, *FEBS Lett.* **1995**, *376*, 1 – 5.
[90] T. Ohnuma, T. Ohnuma, S. Kavy, S. Bhardwaj, J. F. Holland, *Br. J. Cancer* **1980**, *41*, 602 – 608.
[91] J. J. Wilson, S. J. Lippard, *J. Med. Chem.* **2012**, *55*, 5326 – 5336.
[92] Z. Liu, L. Salassa, A. Habtemariam, A. M. Pizarro, G. J. Clarkson, P. J. Sadler, *Inorg. Chem.* **2011**, *50*, 5777 – 5783.
[93] V. Novohradsky, Z. Liu, M. Vojtiskova, P. J. Sadler, V. Brabec, J. Kasparkova, *Metallomics* **2014**, *6*, 682 – 690.

Manuscript received: January 6, 2020
Accepted manuscript online: February 10, 2020
Version of record online: March 10, 2020

 © 2020 Wiley-VCH Verlag GmbH & Co. KGaA, Weinheim